Architectural Editing of Polyesters and Polyurethanes *via* Pd(II)-catalyzed [3,3]-Sigmatropic Oxo-Rearrangements

Rachael A. J. Ditzler[‡,1], Rachel M. Rapagnani[‡,2], Nathaniel K. Berney[1], Ross F. Koby[2], Erin C. Krist[1], Benjamin J. Kruse[1], Hilary D. Fokwa[1], Ian A. Tonks*[,2], and Aleksandr V. Zhukhovitskiy*[,1]

[1]Department of Chemistry, University of North Carolina – Chapel Hill, Chapel Hill, North Carolina 27599, United States

[2]Department of Chemistry, University of Minnesota – Twin Cities, Minneapolis, Minnesota 55455, United States

KEYWORDS. architectural editing, polymer backbone editing, post-polymerization modification, sigmatropic rearrangement, polyester, polyurethane, ethenolysis

ABSTRACT: Architecture underlies the thermomechanical properties of polymers. Yet, few strategies are available to tune a polymer's architecture after it is prepared without altering its chemical composition. The ability to edit the architecture of a polymer would dramatically expand the accessible architecture-property space of polymeric materials. Herein, we disclose a backbone rearrangement approach to tune the short-chain branching of polymers. Specifically, we demonstrate that palladium(II)-catalyzed [3,3]-sigmatropic oxo-rearrangements can transform branched polyesters and polyurethanes to their linear counterparts. While the effects on materials properties are generally subtle in the case of polyesters, more dramatic changes are observed in the case of polyurethanes: two polyurethanes undergo a soluble-to-insoluble transition, and one exhibits a dramatic increase in both strain at break and toughness after rearrangement. Additionally, the incorporation of alkenes in the polymer backbone through the rearrangement enables facile deconstruction *via* ethenolysis. In all, we disclose a powerful and broad-scope strategy to edit the architecture of polymer backbones and thereby tune their physical and chemical properties.

INTRODUCTION

The architecture of polymer backbones underlies their thermomechanical properties, as can be readily observed by comparing high density (linear) and linear low density (short branches) polyethylene.[1] While considerable attention has been devoted over the years to post-polymerization transformations of the global polymer architecture/topology,[2–15] modification of local architecture—specifically, short-chain branching—has received much less attention: typically, the extent of branching is controlled by catalyst design and/or addition of branch-bearing co-monomers, and once formed, the architecture of the polymer backbone is conventionally regarded as immutable.[16–19] In the exceptions, such as mechanochemical ring-openings,[20,21] the chemical functionality of the polymers is fundamentally altered, so the connection between isomeric architectural change and polymer properties is difficult to determine.

Given our interest in the ability to edit polymer backbones—as demonstrated in our previous reports using the Ireland-Claisen rearrangement on polyesters and the anionic Brook rearrangement on poly(acyl silanes) to edit backbone chemical composition[22,23]—we envisioned that this strategy might lend itself well toward architectural modifications to yield isomeric polymers with different backbones. Our aim herein differs from our previous reports: in this work, we seek to modify polymer architecture while maintaining the class to which the polymer belongs—

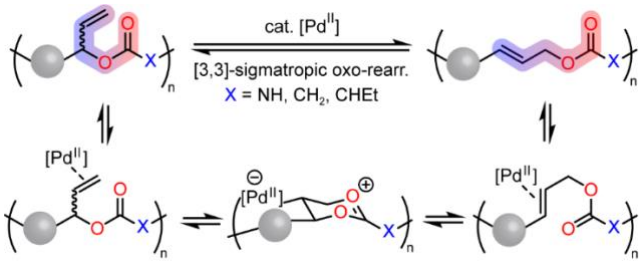

Figure 1. Proposed [3,3]-sigmatropic oxo-rearrangement (SOR) of polyesters and polyurethanes from branched to linear using a Pd(II) catalyst via an acetoxonium intermediate as reported for small molecule esters and carbamates.[24]

e.g., a polyester stays a polyester—and use catalytic reagents instead of stoichiometric ones. Critically, most reported polymer backbone edits are highly backbone-specific, which in turn limits their implementation,[20,25–30] and we sought to address this challenge within the context of architectural editing to ensure broad utility. We identified the transition metal-catalyzed formal [3,3]-sigmatropic oxo-rearrangement (SOR) of allylic esters and carbamates (Figure 1) as a potential candidate transformation for this purpose. Winstein and coworkers first observed this type of rearrangement in 1966 in the context of small molecules containing allylic esters[31] and Henry elucidated its mechanism in 1971.[24] Furthermore, Henry found that palladium(II) salts were the most active among noble metal π-acid catalysts available at the time, and produced evidence for what

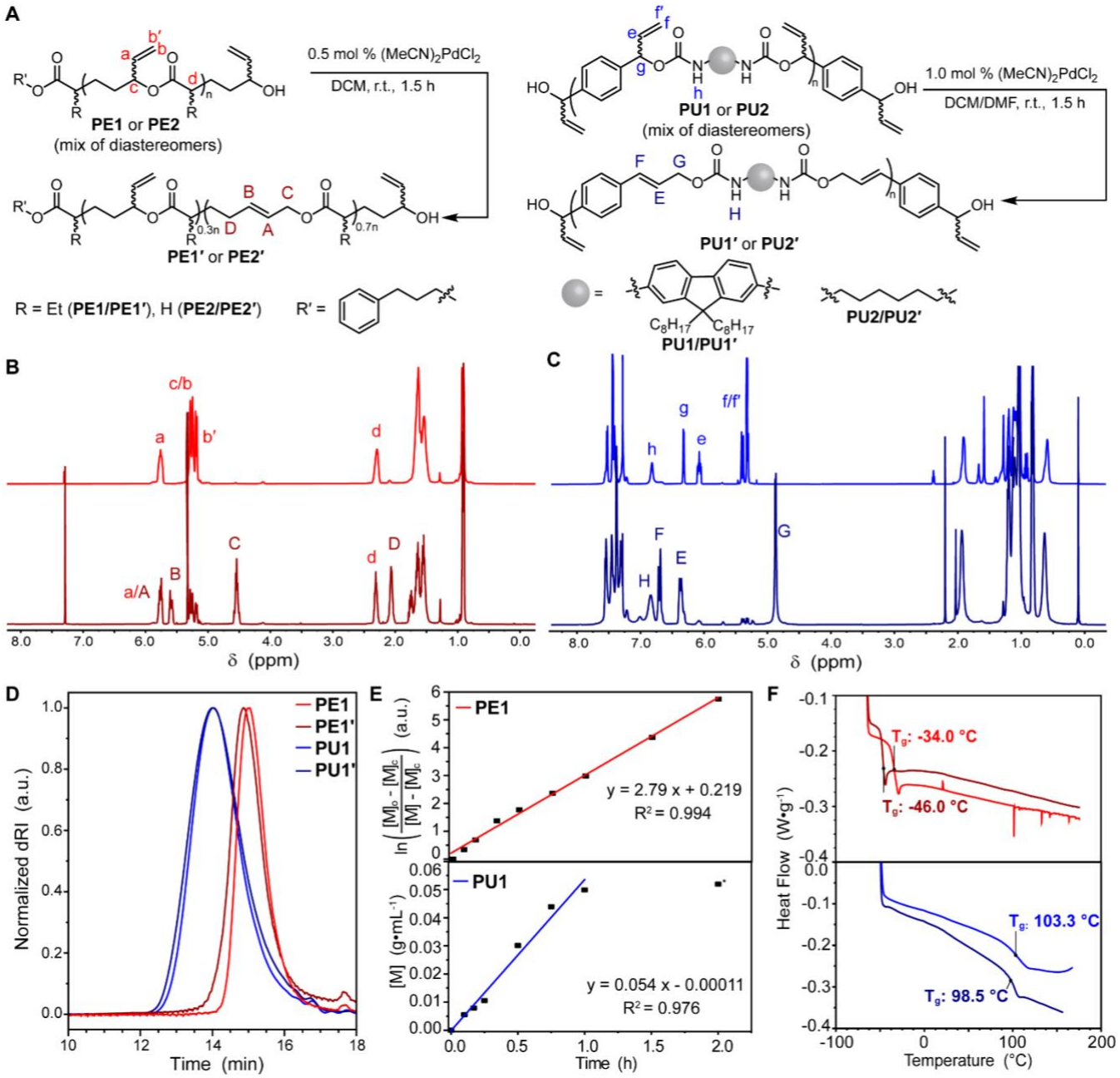

Figure 2. A. SOR of **PE1**, **PE2**, **PU1**, and **PU2**. B. Stacked ^{1}H NMR ($CDCl_3$, 500 MHz, 25 °C) spectra of **PE1** (red) and crude **PE1′** (maroon). C. Stacked ^{1}H NMR ($CDCl_3$, 500 MHz, 25 °C) spectra of **PU1** (blue) and crude **PU1′** (navy). D. Gel-permeation chromatography with multi-angle light scattering (tetrahydrofuran, 35 °C) differential refractive index (dRI) traces of **PE1** (red, M_n = 7.55 kDa, Đ = 1.21, dn/dc = 0.0768), **PE1′** (maroon, M_n = 8.84 kDa, Đ = 1.20, dn/dc = 0.0795), **PU1** (blue, M_n = 22.3 kDa, Đ = 1.66, dn/dc = 0.144), and **PU1′** (navy, M_n = 23.3 kDa, Đ = 1.43, dn/dc = 0.196). E. Semilogarithmic plot of the equilibrium kinetics of the **PE1**-to-**PE1′** rearrangement (red, Figure S46), where equilibrium conversion is set to 0.665 and plot of pseudo zero-order kinetics of the **PU1**-to-**PU1′** rearrangement (blue, Figure S49, * - point excluded as reaction had reached terminal conversion, [M] refers to concentration of **PU1′**). F. Differential scanning calorimetry (DSC) curves before (red, blue) and after (maroon, navy) rearrangement of **PE1** and **PU1,** respectively.

is now the accepted mechanism of the isomerization/equilibration via the formation of a cyclic acetoxonium intermediate.[24] Meyer and then Overman and Knoll each improved upon and expanded the application of this chemistry by using acetonitrile and benzonitrile complexes of $PdCl_2$ as catalysts, which exhibited a factor of 10^{13}–10^{14} rate enhancement of the isomerization compared to the uncatalyzed reaction.[32–36] We envisioned that this catalytic system would prove similarly effective to isomerize branched polyester and polyurethane backbones into linear ones or vice versa, as dictated by thermodynamics.

RESULTS AND DISCUSSION

We selected polyesters **PE1** and **PE2** and polyurethanes **PU1** and **PU2** as our initial substrates (Figure 2A). The polyesters were previously reported by our groups in the

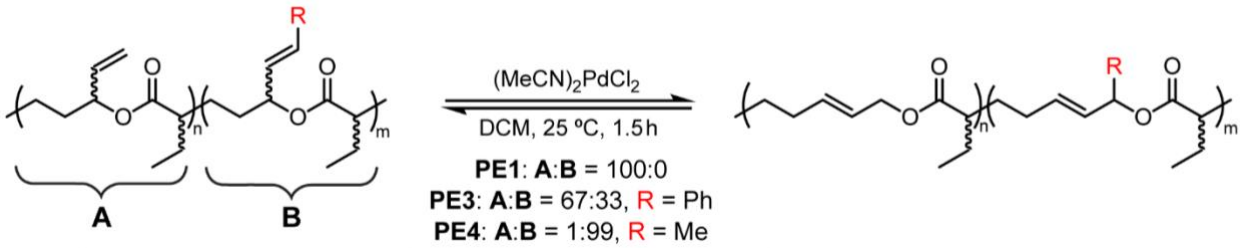

Polym.	$M_{n,i}$ (kg•mol^{-1})	Đ	% rearr. A	% rearr. B	$M_{n,f}$ (kg•mol^{-1})	Đ	$\Delta G_B°$ (kcal•mol^{-1})
PE1	7.55	1.21	68	n/a	8.84	1.20	0.29
PE3	31.6	2.36	70	0	32.5	2.98	3.2
PE4	22.3	1.15	n/a	63	17.7	1.41	0.31

Figure 3. SOR of polyester **PE1** and functionalized polyesters **PE3** and **PE4** (M_n = 14.8 kDa, Đ = 1.11 for **PE1** used in the cross-metathesis reaction to afford **PE3** and **PE4**). % rearr. **A** refers to the rearrangement of the unfunctionalized PE segments; % rearr. **B** refers to the rearrangement of the functionalized PE segments (Figures 2B, 2D, S13–S17, S51–S73); $\Delta G_B°$, the $\Delta G°$ calculated for SOR of segment B, was calculated by DFT computations on one representative monomer unit of each polymer, with a 6-311+g(d,p) basis set and M06-2X functional (See Supplementary Information Computational Procedure and Results).

contexts of using CO_2 and butadiene as sustainable precursors[37] (for **PE1**) and polymer backbone Ireland-Claisen rearrangements (for **PE2**).[22] Notably, these polyesters are differentiated by the α-carbonyl ethyl substituent in **PE1**, which is absent in **PE2**. Meanwhile, polyurethanes **PU1** and **PU2** were designed to ensure solubility, incorporate the allylic carbamate "sigmatropomer", and, in the case of **PU2**, incorporate a commercial diisocyanate. Synthesis of **PE1** (M_n = 7.55 kDa, Đ = 1.21, Figure 2D) and **PE2** (M_n = 7.47 kDa, Đ = 1.07, Figure S1) followed established protocols,[22,37] and **PU1** (M_n = 22.3 kDa, Đ = 1.63, Figures 2D and S2–S6) and **PU2** (M_n = 14.4 kDa, Đ = 1.66, Figures S7–S12) were synthesized via di-*n*-butyltin(IV) dilaurate-catalyzed step-growth copolymerization of 1,4-phenylenebis(2-propen-1-ol) (**3**) and either 9,9-di-*n*-octyl-9H-fluorene-2,7-diisocyanate (**4**) or hexamethylene diisocyanate (HMDI), respectively, in dichloromethane (DCM) at 25 °C for 16 hours.

Subjection of **PE1, PE2, PU1**, and **PU2** to $(MeCN)_2PdCl_2$ led to rapid rearrangement of these polymers from branched to linear (**PE1′, PE2′, PU1′**, and **PU2′**, respectively; Figures 2A and S13–S33). For **PE1** and **PE2**, clean conversion (68.4 ± 0.5% and 75 ± 1%, respectively) was achieved in 1.5 hours based on ^{1}H nuclear magnetic resonance (NMR) spectroscopy (Figures 2B and S13–S22; errors are standard deviations based on 5 and 3 trials, respectively). Fully linear **PE2′** was synthesized independently *via* polycondensation polymerization of methyl (Z)-7-hydroxyhept-5-enoate (**5**, Figures S34–S38) and subjected to the same SOR conditions as **PE2**; this polymer achieved 33% conversion to the branched product **PE2** (Figures S39–S43) as expected based on the conversion of the forward reaction, thus demonstrating the reversible nature of this SOR. For **PU1**, 98% conversion was achieved in <2 hours, also with no side-reactivity (Figures 2C and S23–S27). In contrast, rearrangement of **PU2** proceeded to ~55% conversion by ^{1}H NMR spectroscopy in 20 min, after which precipitation of the polymer was observed (Figure S28). ^{1}H NMR characterization of the precipitated **PU2′** re-dissolved in deuterated dimethyl sulfoxide (DMSO-d_6) revealed a net 89% conversion of branched allylic carbamates to their linear isomers. (Figures S29–S33). Most of the Pd was removed from **PU1′** and **PU2′** during workup and from **PE1′** (Table S1). By gel permeation chromatography with multi-angle light scattering (GPC-MALS), the number-average molecular weights (M_n) of **PE1′**, **PE2′**, and **PU1′** were nearly identical to those of the parent polymers (Figures 2D and S1), which confirms that chain cleavage does not take place, as expected based on the mechanism of SOR (Figure 1). GPC-MALS was not obtained for **PU2′** due to poor solubility in solvents other than DMSO; however, the diffusion-ordered spectroscopy (DOSY) diffusion coefficient for the polymeric species did not change (2.15×10^{-7} cm^2/s, Figures S44–S45), which supports a lack of chain cleavage in this case as well.

Higher conversions in the case of **PE1** and **PE2** could not be reached by varying concentration or catalyst loading, which indicates that isomerization proceeds under thermodynamic control; reaction kinetics are also consistent with first order equilibrium (Figures 2E and S46–S48). Nearly quantitative conversions of **PU1** and **PU2** are likely due to the thermodynamically favored migration of the alkene into conjugation with the benzene ring (Figures 2C and S23–S33). However, surprisingly, rearrangement kinetics for **PU1** and **PU2** are zero order in alkene (Figures 2E, S28, and S49–S50), which is indicative of strong binding of the catalyst to the polymer substrate.

Indeed, ground state DFT calculations on the thermodynamic equilibrium for one representative repeat unit of **PE1**, **PE2**, **PU1**, and **PU2**, capped with methoxy groups or hydrogen atoms for polyurethanes and polyesters, respectively (Figure 3, right column), are consistent with the experimental observations above (Figure 2). The calculated $\Delta G°$ of **PE1** and **PE2** are both close to 0 (0.29 kcal/mol and 0.11 kcal/mol, respectively), consistent with incomplete rearrangement, while **PU1** (-6.9 kcal/mol) and **PU2** (-1.5 kcal/mol) are driven to near-complete conversion based on the stability of the conjugated alkene. Additionally, such simple DFT methods can easily be used to predict the degree of rearrangement of

other polymers (*e.g.* **PE3** and **PE4**, *vide infra*), providing a useful tool for future polymer synthesis and modification.

With this information in hand, we reasoned that alkene sub-

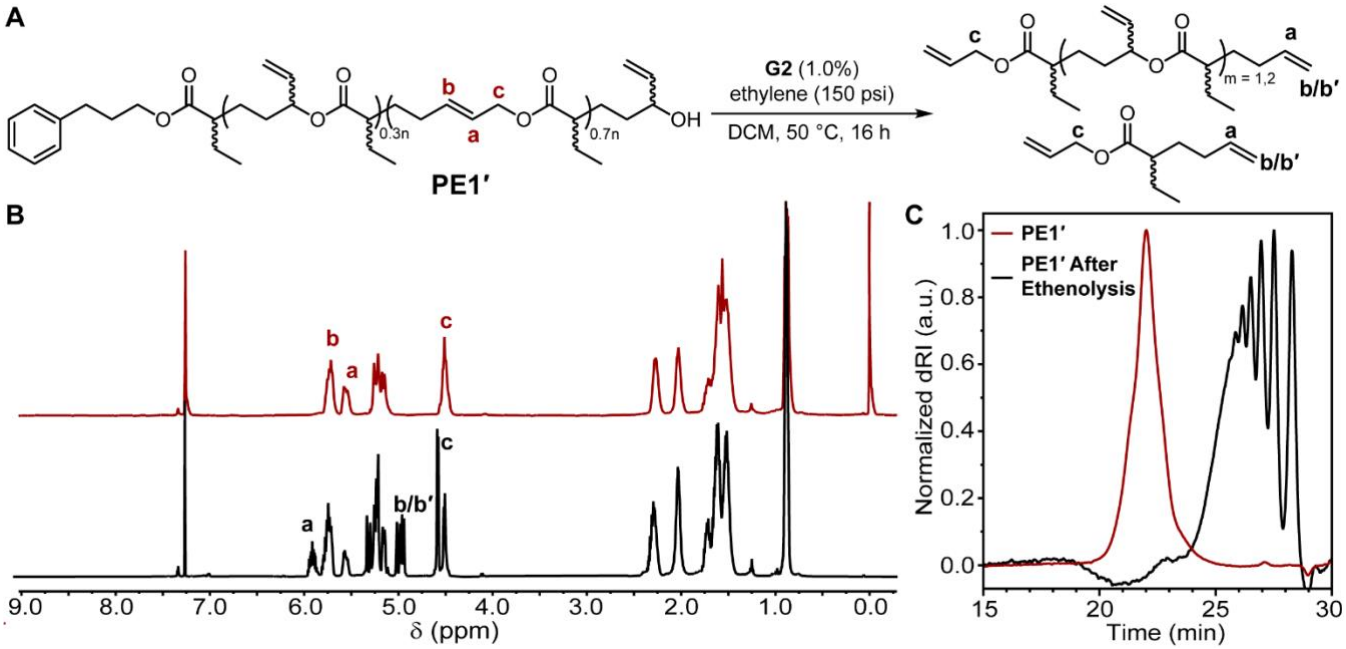

Figure 4. A. SOR and subsequent degradative ethenolysis of **PE1**. B. Stacked ^{1}H NMR spectra of **PE1′** (maroon) and the crude mixture after ethenolysis was performed (black). C. GPC-MALS dRI traces before (maroon, M_n = 22.8 kDa, Đ = 1.39) and after ethenolysis (black, M_n = 0.85 kDa, Đ = 1.25) of **PE1′.**

stitution could be utilized to tune the rearrangement efficiency of polyesters and produce novel materials that could not be easily accessed *via* direct polymerization. To explore these possibilities, cross-metathesis of the parent polyester, **PE1**, was employed with styrene and 2-butene to afford **PE3** and **PE4** respectively (Figures S51–S61). As might be expected, the styrenyl-functionalized esters in **PE3** do not rearrange because the resulting loss of conjugation would be thermodynamically uphill. As an internal control, the non-functionalized (R = H) repeat units in **PE3** underwent 70% rearrangement, consistent with the previously established thermodynamics of the **PE1**-to-**PE1′** rearrangement (Figures 3 and S62–S67). Meanwhile, the propenyl- functionalized esters in **PE4** undergo rearrangement to a similar degree of conversion (63%) as the vinyl-functionalized ones in **PE1** (Figures 3 and S68–S73). Ground state DFT calculations on the thermodynamic equilibrium are consistent with experimental observations for **PE3** and **PE4** as well, with a calculated ΔG° of 3.2 kcal/mol and 0.31 kcal/mol respectively, consistent with no rearrangement and incomplete rearrangement (Figure 3).

Having established the viability of architectural editing, we proceeded to explore its effects on the materials' thermal and mechanical properties. After rearrangement of **PE1** to **PE1′**, the glass transition temperature (T_g) decreased by 12 °C (Figure 2F), which is consistent with reduced branching.[38] Similar decreases in T_g (13 °C, 10 °C, 3 °C, and 5 °C) were observed for **PE2** / **PE2′**, **PE3** / **PE3′**, **PE4** / **PE4′**, and **PU1** / **PU1′**, respectively (Figures S74–S76 and 2F). Although the % conversion to "linear" is higher for **PU1′** compared to all of the polyesters, the smaller shift in T_g than might be expected is most likely due to the dilution of the effects by the unchanged di-*n*-octylfluorene fragments. On the other hand, the T_g of **PU2** observed at 64 °C disappears for **PU2′**—at least it is not observed below the decomposition temperature of **PU2′** ($T_{d,1\%}$ = 195 °C, Figures S77–S78). Increased hydrogen bonding and π-stacking in the more linearized architecture could explain the disappearance of T_g. Powder X-ray diffraction (PXRD) confirms a new chain packing pattern for **PU2′** compared to **PU2** (Figure S79). The major observed peaks for **PU2** and **PU2′** with d-spacings of 4.54 Å and 4.08 Å respectively are consistent with hydrogen bonding between polyurethane chains (Figure S79).[39]

Thermal stabilities of **PE1**–**PE4** and their rearranged counterparts **PE1′**–**PE4′** proved to be nearly identical: for instance, the decomposition temperature at 5% mass loss, $T_{d,5\%}$, of **PE1′** was only 4 °C smaller than that of **PE1** (Figures S80–S83). A similar trend was observed for **PU2** / **PU2′** with post-rearrangement reduction in $T_{d,5\%}$ of 2 °C (Figure S78). Notably, a bigger change in the opposite direction was observed for **PU1** / **PU1′**: $T_{d,5\%}$ of **PU1′** was 31 °C greater than that of **PU1**; however, beyond this first stage, further mass loss for **PU1** and **PU1′** was virtually identical (Figure S84). On the whole, architecture alone appears to have a subtle impact on the thermal stability of isomeric polymers.

Another valuable feature of this rearrangement is the introduction of alkenes into the polymer backbone; for instance, this functionality enables deconstruction *via* ethenolysis.[40,41] Using the parent **PE1** as a model system, we first performed rearrangement under our standard conditions (*vide supra*), and then, without purification, exposed it to 2nd-generation Grubbs catalyst (**G2,** 1 mol %) and ethylene gas (150 psi, 50 °C, 16 hours, Figure 4A). Fragmentation of the polymer backbone was observed by both ^{1}H NMR spectroscopy (Figures 4B and S85–S89) and by a dramatic decrease in M_n by GPC-MALS (Figure 4C). The viability of this procedure demonstrates that $(MeCN)_2PdCl_2$ does not interfere with **G2** during ethenolysis. Additionally, as expected, **PE1** remains unchanged under our standard ethenolysis conditions prior to the rearrangement (Figure

S90). These reaction sequences demonstrate a straightforward way to selectively

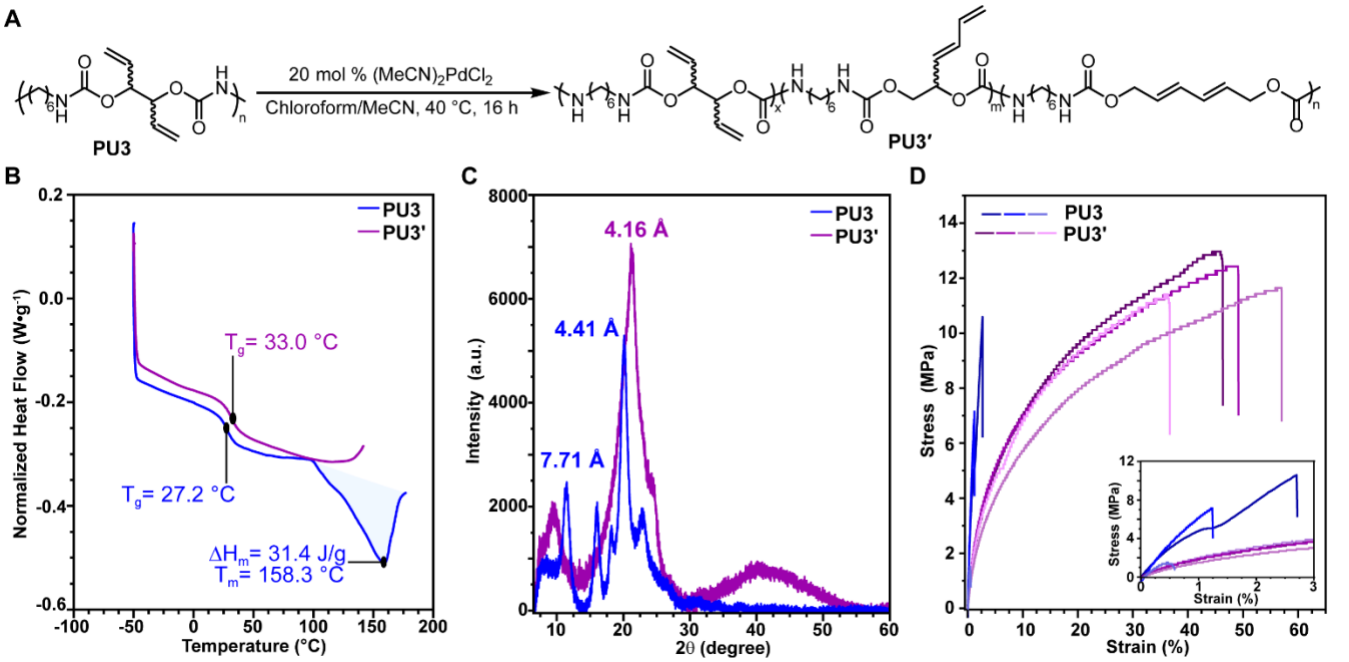

Figure 5. A. SOR of **PU3** to **PU3′** catalyzed by $(MeCN)_2PdCl_2$. B. Differential scanning calorimetry (DSC) curves comparing **PU3** (blue) and **PU3′** (purple); light blue shaded area corresponds to area under the melting peak used to calculate ΔH_m. C. Powder X-ray diffraction (PXRD) of **PU3** (blue) and **PU3′** (purple) with the distance corresponding to the major peak listed. D. Multiple uniaxial tensile test trials for **PU3** (blue hues) and **PU3′** (purple hues).

deconstruct **PE1** through a two-step one-pot reaction sequence, in addition to the previously shown chemical recycling and biodegradation pathways that are possible.[37] Such a sequence could be a valuable tool for the selective deconstruction and separation of **PE1** or other α-vinyl sidechain polyesters in the presence of mixed polyester waste streams, which typically all undergo hydrolysis or catalyzed ring-closing depolymerization and are thus difficult to separate from each other.[42,43]

To demonstrate broader utility of architectural editing, another polyurethane, **PU3** (M_n = 5.05 kDa, Đ = 1.40), was synthesized directly from commercial starting materials 1,5-hexadiene-3,4-diol and HMDI to afford a polymer that both contains the allylic carbamate sigmatropomer and whose production can be readily scaled up (Figures S91–S96). Rearrangement of **PU3** was achieved using 20 mol % $(MeCN)_2PdCl_2$ at 40 °C to afford **PU3′** with ~76% rearranged allylic carbamates, of which 66% formed internal 1,3-dienes, and the other 10%—external 1,3-dienes (Figures 5A and S97–S101). We hypothesize that higher temperatures and catalyst loadings are required for the rearrangement of **PU3** compared to **PU1** and **PU2** because the resulting 1,3-dienes could poison the catalyst.[32,36] Ground state DFT calculations on the thermodynamic equilibrium are consistent with experimental observations for **PU3**, with a calculated ΔG° of -4.4 kcal/mol and -2.9 kcal/mol for formation of the internal 1,3-diene and external 1,3-diene respectively (See Supplementary Information Computational Procedure and Results). Most of the Pd was removed during workup (Table S1). Attempts to achieve higher conversion afforded an insoluble material. GPC-MALS was not obtained for **PU3′** due to poor solubility in solvents other than DMSO; however, DOSY for **PU3** and **PU3′** affords the same diffusion coefficient (3.98×10^{-7} cm^2/s) for the polymeric species (Figures S102–S103). Since **PU3** and **PU3′** have the same diffusion coefficient, we conclude that, as in other cases, this polymer remains intact throughout the SOR.

Compared to **PU1** and **PU2**, rearrangement of **PU3** leads to a substantially reduced $T_{d,5\%}$ in **PU3′** (from 228 °C to 164 °C, Figure S104). Here, too, we think the key culprit is the presence of 1,3-dienes in the product. In addition to decreased thermal stability, **PU3′** has a slightly increased T_g compared to **PU3** (Figure 5B). Furthermore, while **PU3** is a semicrystalline material, **PU3′** is amorphous, as confirmed by both the disappearance of the melting transition in DSC traces and the simultaneous disappearance of some peaks and broadening of others in the PXRD traces (Figures 5B and 5C). The major observed d-spacing for **PU3** and **PU3′** (4.41 Å and 4.16 Å respectively) is consistent with hydrogen bonding between polyurethane chains (Figure 5C).[39]

Uniaxial tensile testing was performed on thin films of **PU3** and **PU3′** at a strain rate of 0.0042 Hz (12 mm sample length, 0.05 mm/s). **PU3′** has a much higher strain at break (47 ± 8 %) and toughness (4.2 ± 0.8 MPa) compared to **PU3** (2 ± 1% and 0.07 ± 0.07 MPa respectively, Figure 5D), but a lower Young's modulus (0.20 ± 0.02 GPa compared to 0.7 ± 0.2 GPa for **PU3**, Figure 5D). Furthermore, **PU3′** exhibits yielding behavior which could be due to facilitated chain slippage in the absence of crystalline domains. In short, the rearrangement leads in this case to a more amorphous and tougher material.

CONCLUSION

We have demonstrated the branched-to-linear architectural editing of a variety of functionalized polyesters and polyurethanes via the Pd(II)-catalyzed [3,3]-sigmatropic oxo-rearrangement. This transformation affords polyesters and polyurethanes with thermodynamically-controlled

degrees of branching. Subtle material property shifts were observed for all tested polyesters, however the impact of the branched-to-linear architectural edit in polyurethanes afforded more dramatic shifts; namely a decrease in solubility and for one material, a dramatic increase in toughness and strain at break. Inclusion of the pendent alkene into the polymer backbone lends itself to a two-step, one-pot, facile deconstruction of polyesters via ethenolysis with the potential to be applied towards polyurethane deconstruction. More broadly, our approach increases the generality of polymer backbone editing and opens the door to wider application across multiple classes of materials.

ASSOCIATED CONTENT

Supporting Information.
The Supporting Information is available free of charge via the Internet at http://pubs.acs.org.

Materials and methods, synthetic and characterization procedures, supplementary text and figures, and spectral data (PDF).

AUTHOR INFORMATION

Corresponding Authors

Ian A. Tonks – *Department of Chemistry, University of Minnesota – Twin Cities, Minneapolis, Minnesota 55455, United States; orcid.org/0000-0001-8451-8875;*
Email: **itonks@umn.edu**

Aleksandr V. Zhukhovitskiy – *Department of Chemistry, University of North Carolina – Chapel Hill, Chapel Hill, North Carolina 27599, United States; orcid.org/0000-0002-3873-4179;*
Email: **alexzhuk@email.unc.edu**

Authors

Rachael A. J. Ditzler – *Department of Chemistry, University of North Carolina – Chapel Hill, Chapel Hill, North Carolina 27599, United States; orcid.org/0000-0002-1390-9841*

Rachel M. Rapagnani – *Department of Chemistry, University of Minnesota – Twin Cities, Minneapolis, Minnesota 55455, United States; orcid.org/0000-0003-1688-3162*

Nathaniel K. Berney – *Department of Chemistry, University of North Carolina – Chapel Hill, Chapel Hill, North Carolina 27599, United States; orcid.org/0009-0004-8565-3226*

Ross F. Koby – *Department of Chemistry, University of Minnesota – Twin Cities, Minneapolis, Minnesota 55455, United States; orcid.org/0000-0001-5394-1160*

Erin C. Krist – *Department of Chemistry, University of North Carolina – Chapel Hill, Chapel Hill, North Carolina 27599, United States; orcid.org/0000-0002-6498-9175*

Benjamin J. Kruse – *Department of Chemistry, University of North Carolina – Chapel Hill, Chapel Hill, North Carolina 27599, United States; orcid.org/0009-0003-2850-143X*

Hilary D. Fokwa – *Department of Chemistry, University of North Carolina – Chapel Hill, Chapel Hill, North Carolina 27599, United States; orcid.org/0000-0003-4021-1294*

Author Contributions

‡These authors contributed equally.

Notes

I.A.T. and R.M.R. are co-inventors on a provisional US patent covering the methods of polymerization and composition of matter for **PE1** presented in this work, filed through the University of Minnesota (application no. 63/156,135). A.V.Z., I.A.T., R.A.J.D., R.M.R, and N.K.B are all co-inventors on a provisional US patent covering the methods of rearrangement and composition of matter presented in this work, filed through the University of Minnesota and the University of North Carolina at Chapel Hill (application no. 63/470,748). R.F.K., E.C.K., B.J.K., and H.D.F. declare no competing interests.

ACKNOWLEDGMENTS

This material is based on work supported by the National Science Foundation under Grant No. DGE-1650116 (Graduate Research Fellowship for R.A.J.D.) and Grant No. 1828183 (NMR instrument grant at UNC). Any opinions, findings, and conclusions or recommendations expressed in this material are those of the author(s) and do not necessarily reflect the views of the National Science Foundation. Funding for this work at UNC-CH was provided by the Army Research Office Young Investigator Program (Award No. W911NF-23-1-0265). The research work conducted by B.J.K. was supported by the DoD NDSEG Fellowship. Funding for this work at UMN was provided by the NSF Center for Sustainable Polymers (no. CHE-1901635 to I.A.T.) at the University of Minnesota as well as the University of Minnesota Doctoral Dissertation Fellowship (to R.M.R.). Instrumentation for the University of Minnesota Chemistry NMR facility was supported by a grant through the National Institutes of Health (no. S10OD011952). This work was performed in part at the Chapel Hill Analytical and Nanofabrication Laboratory, CHANL, a member of the North Carolina Research Triangle Nanotechnology Network, RTNN, which is supported by the National Science Foundation, Grant ECCS-2025064, as part of the National Nanotechnology Coordinated Infrastructure, NNCI. We thank the UNC-CH Department of Chemistry NMR Core Laboratory for the use of their NMR spectrometers and the Chapel Hill Analytical and Nanofabrication Laboratory (CHANL) for use of their X-ray diffractometer. We acknowledge the Minnesota Supercomputing Institute (MSI) at the University of Minnesota for providing resources that contributed to the research results reported within this paper. URL: http://www.msi.umn.edu. We thank Michael Harris and Andrew Puente for their assistance with running calculations. We thank the Leibfarth group (UNC-CH, Chemistry) for the use of their Instron and DSC instruments. We also thank the You group (UNC-CH, Chemistry) for the use of their TGA instrument and the Dingemans group (UNC-CH, Applied Physical Sciences) for the use of their melt press.

REFERENCES

(1) DeSimone, J. M. Branching Out into New Polymer Markets. *Science* **1995**, *269* (5227), 1060–1061. https://doi.org/10.1126/science.269.5227.1060.

(2) Sun, H.; Kabb, C. P.; Dai, Y.; Hill, M. R.; Ghiviriga, I.; Bapat, A. P.; Sumerlin, B. S. Macromolecular Metamorphosis via Stimulus-Induced Transformations of Polymer Architecture. *Nat. Chem.* **2017**, *9* (8), 817–823. https://doi.org/10.1038/nchem.2730.

(3) Sun, H.; Kabb, C. P.; Sims, M. B.; Sumerlin, B. S. Architecture-Transformable Polymers: Reshaping the Future of Stimuli-Responsive Polymers. *Prog. Polym. Sci.* **2019**, *89*, 61–75. https://doi.org/10.1016/j.progpolymsci.2018.09.006.

(4) Endo, K. Synthesis and Properties of Cyclic Polymers. In *New Frontiers in Polymer Synthesis*; Kobayashi, S., Ed.; Springer Berlin Heidelberg: Berlin, Heidelberg, 2008; pp 121–183. https://doi.org/10.1007/12_2008_157.

(5) De Bo, G.; De Winter, J.; Gerbaux, P.; Fustin, C. Rotaxane-Based Mechanically Linked Block Copolymers. *Angew. Chem. Int. Ed.* **2011**, *50* (39), 9093–9096. https://doi.org/10.1002/anie.201103716.

(6) Schappacher, M.; Deffieux, A. Reversible Switching between Linear and Ring Polystyrenes Bearing Porphyrin End Groups. *J. Am. Chem. Soc.* **2011**, *133* (6), 1630–1633. https://doi.org/10.1021/ja108821p.

(7) Tezuka, Y. *Topological Polymer Chemistry: Progress of Cyclic Polymers in Syntheses, Properties and Functions*; World Scientific, 2013. https://doi.org/10.1142/8443.

(8) Ogawa, T.; Nakazono, K.; Aoki, D.; Uchida, S.; Takata, T. Effective Approach to Cyclic Polymer from Linear Polymer: Synthesis and Transformation of Macromolecular [1]Rotaxane. *ACS Macro Lett.* **2015**, *4* (4), 343–347. https://doi.org/10.1021/acsmacrolett.5b00067.

(9) Ogawa, T.; Usuki, N.; Nakazono, K.; Koyama, Y.; Takata, T. Linear–Cyclic Polymer Structural Transformation and Its Reversible Control Using a Rational Rotaxane Strategy. *Chem. Commun.* **2015**, *51* (26), 5606–5609. https://doi.org/10.1039/C4CC08982K.

(10) Tezuka, Y. Topological Polymer Chemistry Designing Complex Macromolecular Graph Constructions. *Acc. Chem. Res.* **2017**, *50* (11), 2661–2672. https://doi.org/10.1021/acs.accounts.7b00338.

(11) Gu, Y.; Alt, E. A.; Wang, H.; Li, X.; Willard, A. P.; Johnson, J. A. Photoswitching Topology in Polymer Networks with Metal–Organic Cages as Crosslinks. *Nature* **2018**, *560* (7716), 65–69. https://doi.org/10.1038/s41586-018-0339-0.

(12) Mohanty, A. K.; Ye, J.; Ahn, J.; Yun, T.; Lee, T.; Kim, K.; Jeon, H. B.; Chang, T.; Paik, H. Topologically Reversible Transformation of Tricyclic Polymer into Polyring Using Disulfide/Thiol Redox Chemistry. *Macromolecules* **2018**, *51* (14), 5313–5322. https://doi.org/10.1021/acs.macromol.8b00714.

(13) Miao, W.; Zou, W.; Jin, B.; Ni, C.; Zheng, N.; Zhao, Q.; Xie, T. On Demand Shape Memory Polymer via Light Regulated Topological Defects in a Dynamic Covalent Network. *Nat. Commun.* **2020**, *11* (1), 4257. https://doi.org/10.1038/s41467-020-18116-1.

(14) Takata, T. Switchable Polymer Materials Controlled by Rotaxane Macromolecular Switches. *ACS Cent. Sci.* **2020**, *6* (2), 129–143. https://doi.org/10.1021/acscentsci.0c00002.

(15) Zou, W.; Jin, B.; Wu, Y.; Song, H.; Luo, Y.; Huang, F.; Qian, J.; Zhao, Q.; Xie, T. Light-Triggered Topological Programmability in a Dynamic Covalent Polymer Network. *Sci. Adv.* **2020**, *6* (13), eaaz2362. https://doi.org/10.1126/sciadv.aaz2362.

(16) Guan, Z.; Cotts, P. M.; McCord, E. F.; McLain, S. J. Chain Walking: A New Strategy to Control Polymer Topology. *Science* **1999**, *283* (5410), 2059–2062. https://doi.org/10.1126/science.283.5410.2059.

(17) Guan, Z. Control of Polymer Topology by Chain-Walking Catalysts. *Chem. Eur. J.* **2002**, *8* (14), 3086–3092. https://doi.org/10.1002/1521-3765(20020715)8:14%3C3086::AID-CHEM3086%3E3.0.CO;2-L.

(18) Arriola, D. J.; Carnahan, E. M.; Hustad, P. D.; Kuhlman, R. L.; Wenzel, T. T. Catalytic Production of Olefin Block Copolymers via Chain Shuttling Polymerization. *Science* **2006**, *312* (5774), 714–719. https://doi.org/10.1126/science.1125268.

(19) Chum, P. S.; Swogger, K. W. Olefin Polymer Technologies—History and Recent Progress at The Dow Chemical Company. *Prog. Polym. Sci.* **2008**, *33* (8), 797–819. https://doi.org/10.1016/j.progpolymsci.2008.05.003.

(20) Potisek, S. L.; Davis, D. A.; Sottos, N. R.; White, S. R.; Moore, J. S. Mechanophore-Linked Addition Polymers. *J. Am. Chem. Soc.* **2007**, *129* (45), 13808–13809. https://doi.org/10.1021/ja076189x.

(21) Chen, Z.; Mercer, J. A. M.; Zhu, X.; Romaniuk, J. A. H.; Pfattner, R.; Cegelski, L.; Martinez, T. J.; Burns, N. Z.; Xia, Y. Mechanochemical Unzipping of Insulating Polyladderene to Semiconducting Polyacetylene. *Science* **2017**, *357* (6350), 475–479. https://doi.org/10.1126/science.aan2797.

(22) Ditzler, R. A. J.; Zhukhovitskiy, A. V. Sigmatropic Rearrangements of Polymer Backbones: Vinyl Polymers from Polyesters in One Step. *J. Am. Chem. Soc.* **2021**, *143* (48), 20326–20331. https://doi.org/10.1021/jacs.1c09657.

(23) Ratushnyy, M.; Zhukhovitskiy, A. V. Polymer Skeletal Editing via Anionic Brook Rearrangements. *J. Am. Chem. Soc.* **2021**, *143* (43), 17931–17936. https://doi.org/10.1021/jacs.1c06860.

(24) Henry, P. M. A Novel Palladium(II) Catalysed Allylic Isomerization. *J. Chem. Soc. D* **1971**, No. 7, 328. https://doi.org/10.1039/c29710000328.

(25) Ditzler, R. A. J.; King, A. J.; Towell, S. E.; Ratushnyy, M.; Zhukhovitskiy, A. V. Editing of Polymer Backbones. *Nat. Rev. Chem.* **2023**, *7* (9), 600–615. https://doi.org/10.1038/s41570-023-00514-w.

(26) Kosaka, N.; Hiyama, T.; Nozaki, K. Baeyer–Villiger Oxidation of an Optically Active 1,4-Polyketone. *Macromolecules* **2004**, *37* (12), 4484–4487. https://doi.org/10.1021/ma0359638.

(27) Aravindu, K.; Cloutet, E.; Brochon, C.; Hadziioannou, G.; Vignolle, J.; Robert, F.; Taton, D.; Landais, Y. Poly(Arylene Vinylene) Synthesis via a Precursor Step-Growth Polymerization Route Involving the Ramberg–Bäcklund Reaction as a Key Post-Chemical Modification Step. *Macromolecules* **2018**, *51* (15), 5852–5862. https://doi.org/10.1021/acs.macromol.8b00676.

(28) Galan, N. J.; Brantley, J. N. General Access to Allene-Containing Polymers Using the Skattebøl Rearrangement. *ACS Macro Lett.* **2020**, *9* (11), 1662–1666. https://doi.org/10.1021/acsmacrolett.0c00745.

(29) Wu, D.; Lenhardt, J. M.; Black, A. L.; Akhremitchev, B. B.; Craig, S. L. Molecular Stress Relief through a Force-Induced Irreversible Extension in Polymer Contour Length. *J. Am. Chem. Soc.* **2010**, *132* (45), 15936–15938. https://doi.org/10.1021/ja108429h.

(30) Porter, M. R. The Nitrosation of Nylon. *J. Polym. Sci.* **1958**, *33* (126), 447–455. https://doi.org/10.1002/pol.1958.1203312641.

(31) Kitching, W.; Rappoport, Z.; Winstein, S.; Young, W. G. Allylic Oxidation of Olefins by Palladium Acetate. *J. Am. Chem. Soc.* **1966**, *88* (9), 2054–2055. https://doi.org/10.1021/ja00961a043.
(32) Overman, L. E. Mercury(II)- and Palladium(II)-Catalyzed [3,3]-Sigmatropic Rearrangements [New Synthetic Methods (46)]. *Angew. Chem. Int. Ed. Engl.* **1984**, *23* (8), 579–586. https://doi.org/10.1002/anie.198405791.
(33) Overman, L. E.; Campbell, C. B.; Knoll, F. M. Mild Procedures for Interconverting Allylic Oxygen Functionality. Cyclization-Induced [3,3] Sigmatropic Rearrangement of Allylic Carbamates. *J. Am. Chem. Soc.* **1978**, *100* (15), 4822–4834. https://doi.org/10.1021/ja00483a032.
(34) Knoll, F. M. The Catalysis of [3,3]-Sigmatropic Rearrangements, University of California, Irvine, Irvine, CA, 1979.
(35) Oehlschlager, C.; Mishra, P.; Dhami, S. Metal-Catalyzed Rearrangements of Allylic Esters. *Can. J. Chem.* **1984**, *62* (4), 791–797. https://doi.org/10.1139/v84-132.
(36) Overman, L. E.; Knoll, F. M. Palladium (II) - Catalyzed Rearrangement of Allylic Acetates. *Tetrahedron Lett.* **1979**, *20* (4), 321–324. https://doi.org/10.1016/S0040-4039(01)85960-8.
(37) Rapagnani, R. M.; Dunscomb, R. J.; Fresh, A. A.; Tonks, I. A. Tunable and Recyclable Polyesters from CO_2 and Butadiene. *Nat. Chem.* **2022**, *14* (8), 877–883. https://doi.org/10.1038/s41557-022-00969-2.
(38) Hiemenz, P. C.; Lodge, T. *Polymer Chemistry*, 2nd ed.; CRC Press: Boca Raton, 2007.
(39) Khanna, S.; Moniruzzaman, M.; Sundararajan, P. R. Influence of Single versus Double Hydrogen-Bonding Motif on the Crystallization and Morphology of Self-Assembling Carbamates with Alkyl Side Chains: Model System for Polyurethanes. *J. Phys. Chem. B* **2006**, *110* (31), 15251–15260. https://doi.org/10.1021/jp0619843.
(40) Conk, R. J.; Hanna, S.; Shi, J. X.; Yang, J.; Ciccia, N. R.; Qi, L.; Bloomer, B. J.; Heuvel, S.; Wills, T.; Su, J.; Bell, A. T.; Hartwig, J. F. Catalytic Deconstruction of Waste Polyethylene with Ethylene to Form Propylene. *Science* **2022**, *377* (6614), 1561–1566. https://doi.org/10.1126/science.add1088.
(41) Bidange, J.; Fischmeister, C.; Bruneau, C. Ethenolysis: A Green Catalytic Tool to Cleave Carbon–Carbon Double Bonds. *Chem. Eur. J.* **2016**, *22* (35), 12226–12244. https://doi.org/10.1002/chem.201601052.
(42) Weng, Y.; Hong, C.-B.; Zhang, Y.; Liu, H. Catalytic Depolymerization of Polyester Plastics toward Closed-Loop Recycling and Upcycling. *Green Chem.* **2024**, *26*, 571-592. 10.1039.D3GC04174C. https://doi.org/10.1039/D3GC04174C.
(43) Cederholm, L.; Olsén, P.; Hakkarainen, M.; Odelius, K. Chemical Recycling to Monomer: Thermodynamic and Kinetic Control of the Ring-Closing Depolymerization of Aliphatic Polyesters and Polycarbonates. *Polym. Chem.* **2023**, *14* (28), 3270–3276. https://doi.org/10.1039/D3PY00535F.

SYNOPSIS TOC